

Computer Modeling of crystalline electrolytes – Lithium Thiophosphates and Phosphates ^a

Nicholas Lepley and N. A. W. Holzwarth

Department of Physics, Wake Forest University, Winston-Salem, NC, USA

- Motivation for solid electrolytes and Li (thio)phosphate materials
- Computational methods
- Li (thio)phosphate crystalline forms and relative stabilities
- Modeling of lithium ion migration in crystalline $\text{Li}_7\text{P}_3\text{S}_{11}$.
- Summary and conclusions

^aSupported by NSF grants DMR-0427055 and 0705239; WFU's DEAC computer cluster.

Solid vs liquid electrolytes in Li ion batteries

Solid electrolytes

Advantages

1. Excellent chemical and physical stability.
2. Performs well as thin film ($\approx 1\mu$).
3. Li^+ conduction only (excludes electrons).

Disadvantages

1. Thin film geometry provides poor contact area for high capacity electrodes.
2. Subject to interface stress if electrodes change size during charge and discharge cycles.
3. Relatively low conductivity per unit area.

Liquid electrolytes

Advantages

1. Excellent contact area with high capacity electrodes.
2. Can accommodate size changes of electrodes during charge and discharge cycles.
3. Relatively high conductivity per unit area.

Disadvantages

1. Relatively poor physical and chemical stability.
2. Relies on the formation of “solid electrolyte interface” (SEI) layer.
3. May have both Li^+ and electron conduction.

Example of solid electrolyte – thin film battery technology

A. Patil et al. / Materials Research Bulletin 43 (2008) 1913–1942

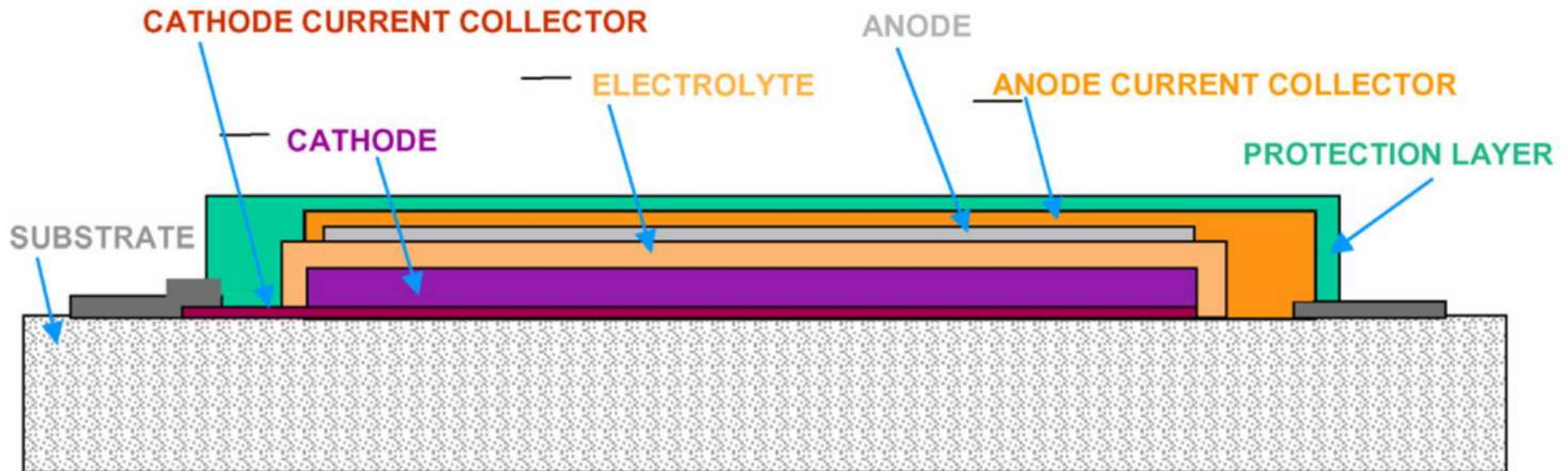


Fig. 2. Schematic cross-section of a thin film lithium battery structure.

Li phosphate (phosphorus oxinitride) (LiPON) and Li thiophosphate electrolytes

LiPON

- Developed at Oak Ridge National Laboratory¹
- Composition: $\text{Li}_x\text{PO}_y\text{N}_z$ with $x = 2y + 3z - 5$, typically $\text{Li}_{2.98}\text{PO}_{3.3}\text{N}_{0.46}$; non-crystalline
- Li^+ conductivity $\sigma \approx 10^{-6}$ S/cm; thermal activation energies 0.3-0.7 eV.

¹ Bates *et al*, *Solid State Ionics* **53-56** 647-654 (1992); Dudney, *Interface* **17(3)** 44-48 (2008)

$\text{Li}_2\text{S-P}_2\text{S}_5$

- Developed at Osaka Prefecture University²
- Composition: Li_xPS_y often with $x = 2y - 5$ (but not always), typically $\text{Li}_{7/3}\text{PS}_{11/3}$; ceramic
- Li^+ conductivity $\sigma \approx 10^{-3}$ S/cm; thermal activation energies 0.1-0.3 eV.

² Mizuno *et al*, *Electrochem. Solid-State Lett.* **8** 918-921 (2005); Hayashi *et al*, *J. Non-Cryst. Solids* **355** 1919-1923 (2009)

LiPON and LiS₂-P₂S₅ conductivities

X. Yu, J. B. Bates, G. E. Jellison, Jr., and F. X. Hart, J. Electrochem. Soc. **144** 524-532 (1997):

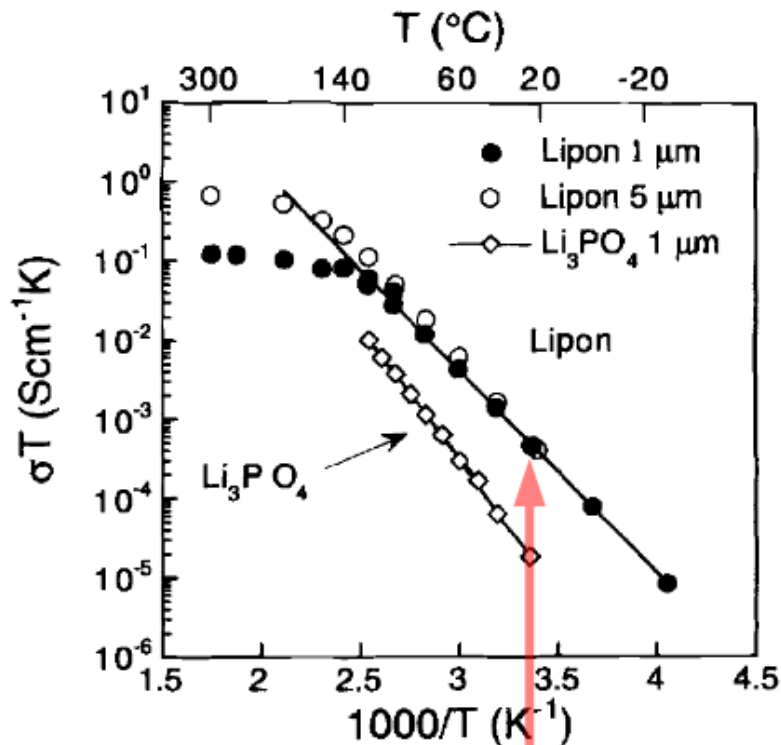


Fig. 3. Arrhenius plot of ionic conductivity of Lipon and Li₃PO₄ vs. temperature.

$$\sigma = 2 \times 10^{-6} \text{ S/cm}$$

$$E_a = 0.5 \text{ eV}$$

M. Tatsumisago and A. Hayashi, J. Non-Cryst. Solids **354** 1411-1417 (2008):

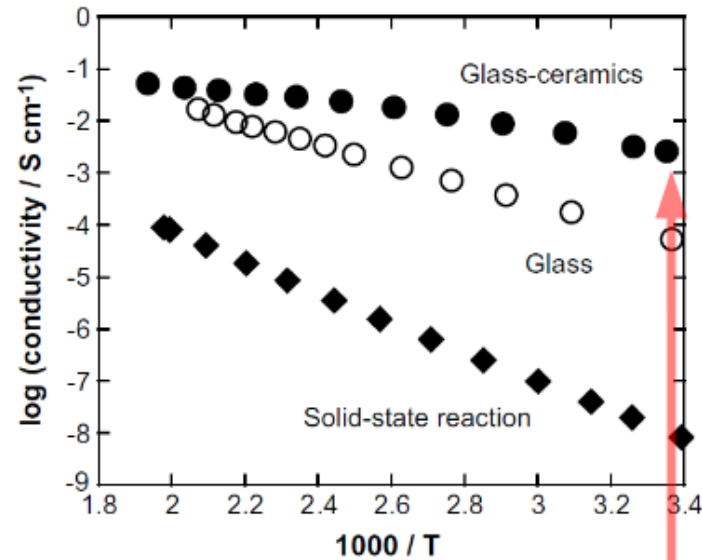


Fig. 5. Temperature dependences of the conductivities for the 70Li₂S · 30P₂S₅ glass and glass-ceramics. The conductivity data for the sample prepared by solid-state reaction are also shown.

$$\sigma = 3 \times 10^{-3} \text{ S/cm}$$

$$E_a = 0.1 \text{ eV}$$

Computational methods

- “First principles” simulations using density functional theory^a to treat the electrons and the Born-Oppenheimer approximation to treat the nuclear positions $\{\mathbf{R}^a\}$, to determine the “total energy” $E(\{\mathbf{R}^a\})$ of the system.
- Variety of computer codes – PWscf^b, pwpaw^c, abinit^d

Results – Quantities derived from $\min_{\{\mathbf{R}^a\}} E(\{\mathbf{R}^a\})$:

- Stable and meta-stable structures
- Heats of formation (ΔH) and possible reactions
- Energies for ion migration (E_m) and for interstitial-vacancy pair formation (E_f) within the “Nudged Elastic Band” (NEB) method [Hankelman *et al*, *JCP* **113** 9901-9904 and 9978-9985 (2000)]

^aHohenberg and Kohn, *Phys. Rev.*, **136** B864 (1964); Kohn and Sham, *Phys. Rev.*, **140** A1133 (1965); using local density approximation (LDA) (Perdew and Wang, *Phys. Rev. B*, **45** 13244 (1992))

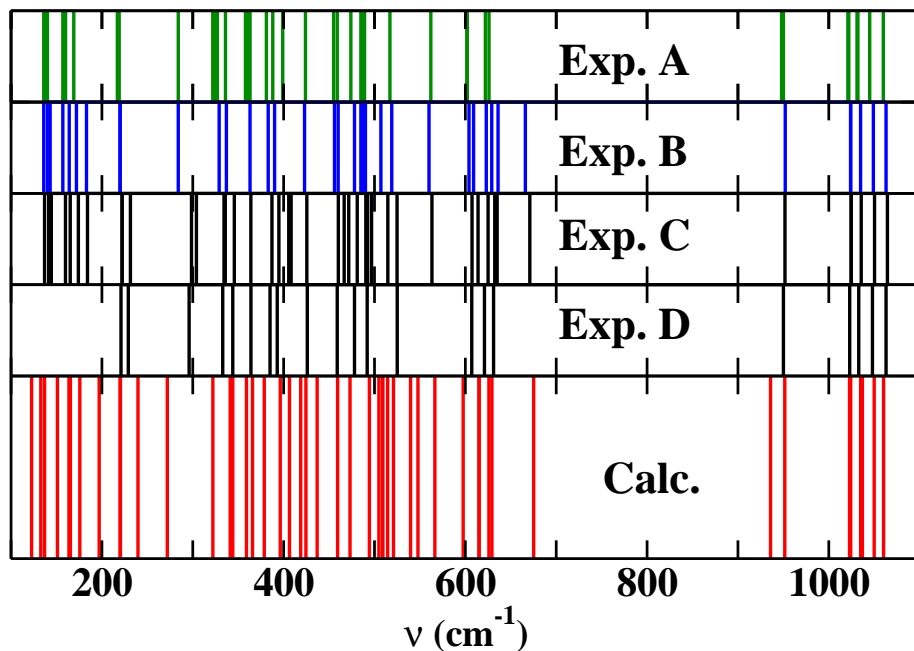
^bGiannozzi *et al*, *J. Phys.: Condens. Matter* **21** 394402 (2009) www.quantum-espresso.org

^cTackett *et al*, *Comp. Phys. Comm.* **135** 348 (2001) pwpaw.wfu.edu

^dGonze *et al*, *Zeit. Kristallogr.* **220** 550 (2005) www.abinit.org.

Computational methods – validation

Raman spectra for γ -Li₃PO₄



Calculated Raman spectra (red) compared with

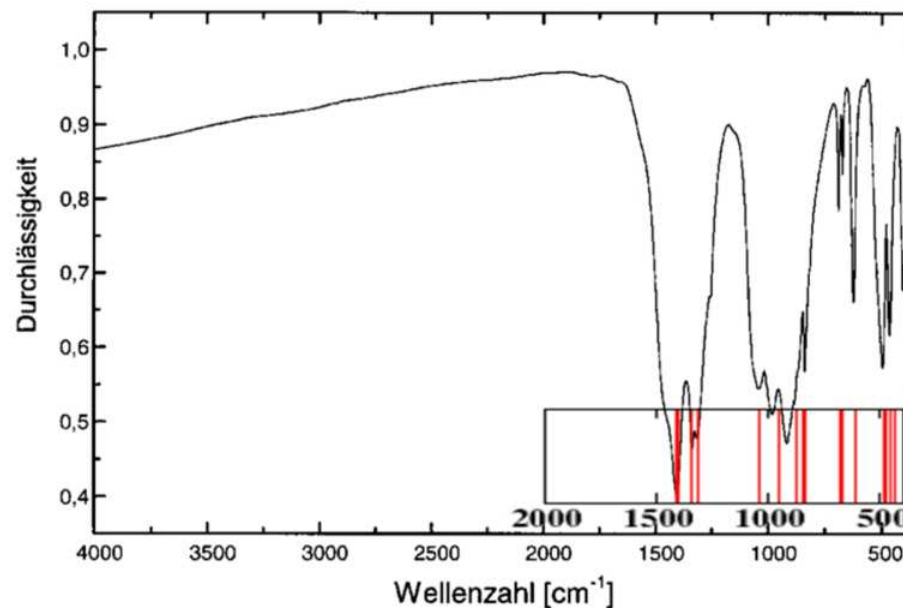
Exp. A: (RT) Mavrin & co-workers, *JETP* **96**, 53 (2003)

Exp. B: (RT) Harbach & co-workers, *Phys. Stat. Sol. B* **66**, 237 (1974)

Exp. C: (LNT) Harbach & co-workers, *Phys. Stat. Sol. B* **66**, 237 (1974)

Exp. D: (LNT) Popović & co-workers, *J. Raman Spec.* **34** 77, (2003)

Infrared spectra for α -P₃N₅



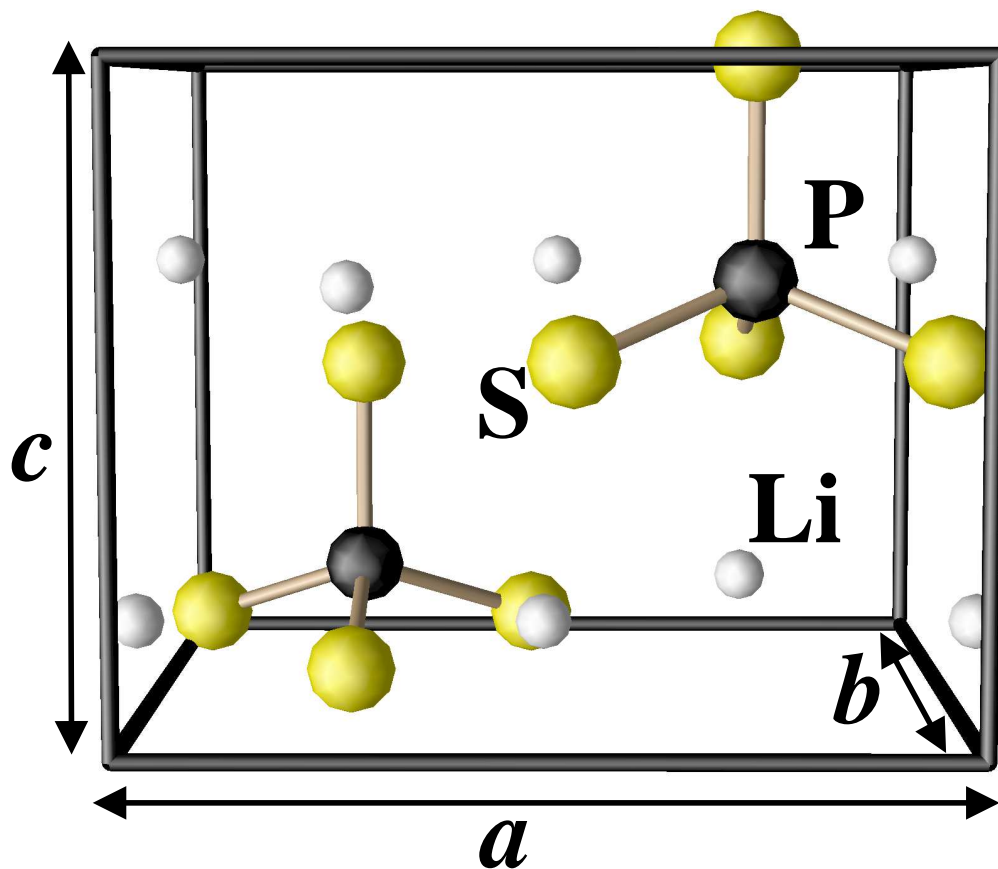
Calculated infrared spectra (red) compared with experiment of Horstmann, Irran, and Schnick, *Z. Anorg. Allg. Chem* **624** 620 (1998).

Heats of formation ΔH_{cal} (eV per formula unit) calculated for the lithium (thio)phosphate and related materials, comparing USPP, PAW and experiment (CRC or NIST).

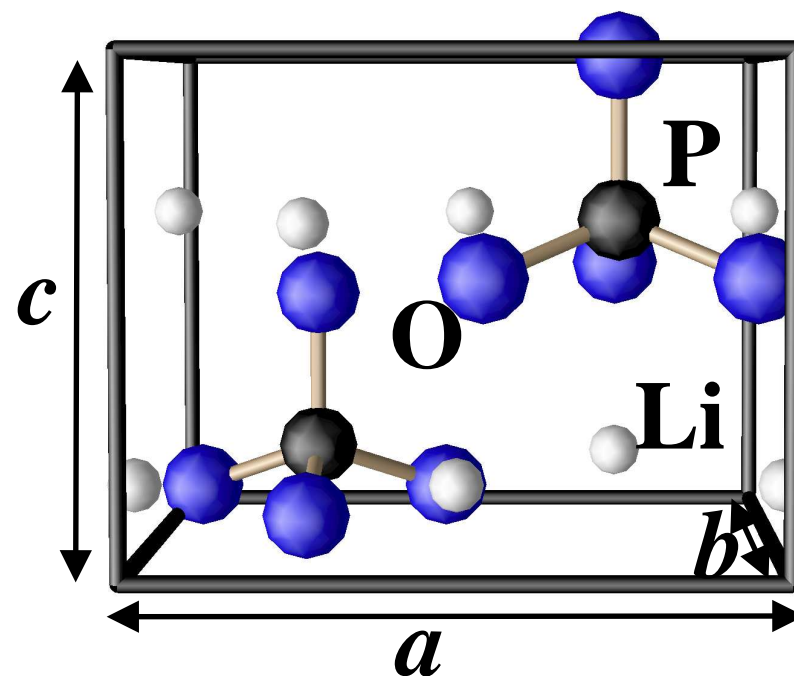
Material	(USPP)	(PAW)	exp
Li ₂ O	-6.18	-6.19	-6.20
Li ₂ O ₂	-6.53	-6.52	-6.57
β -Li ₃ PO ₄	-21.41	-21.39	
γ -Li ₃ PO ₄	-21.38	-21.36	-21.72
Li ₄ P ₂ O ₆	-30.02	-29.93	
Li ₄ P ₂ O ₇	-34.25	-34.21	
Li ₇ P ₃ O ₁₁	-55.26	-55.26	
Li ₂ S	-4.30	-4.30	-4.57
Li ₂ S ₂	-4.10	-4.10	
β -Li ₃ PS ₄	-8.39	-8.35	
γ -Li ₃ PS ₄	-8.19	-8.16	
Li ₄ P ₂ S ₆	-12.45	-12.38	
Li ₄ P ₂ S ₇	-11.62	-11.54	
Li ₇ P ₃ S ₁₁	-20.06	-19.94	
SO ₃	-4.83	-4.86	-4.71
Li ₂ SO ₄	-14.74	-14.76	-14.89

Structural Motifs – Li_3PS_4 and Li_3PO_4

$\beta\text{-Li}_3\text{PS}_4$

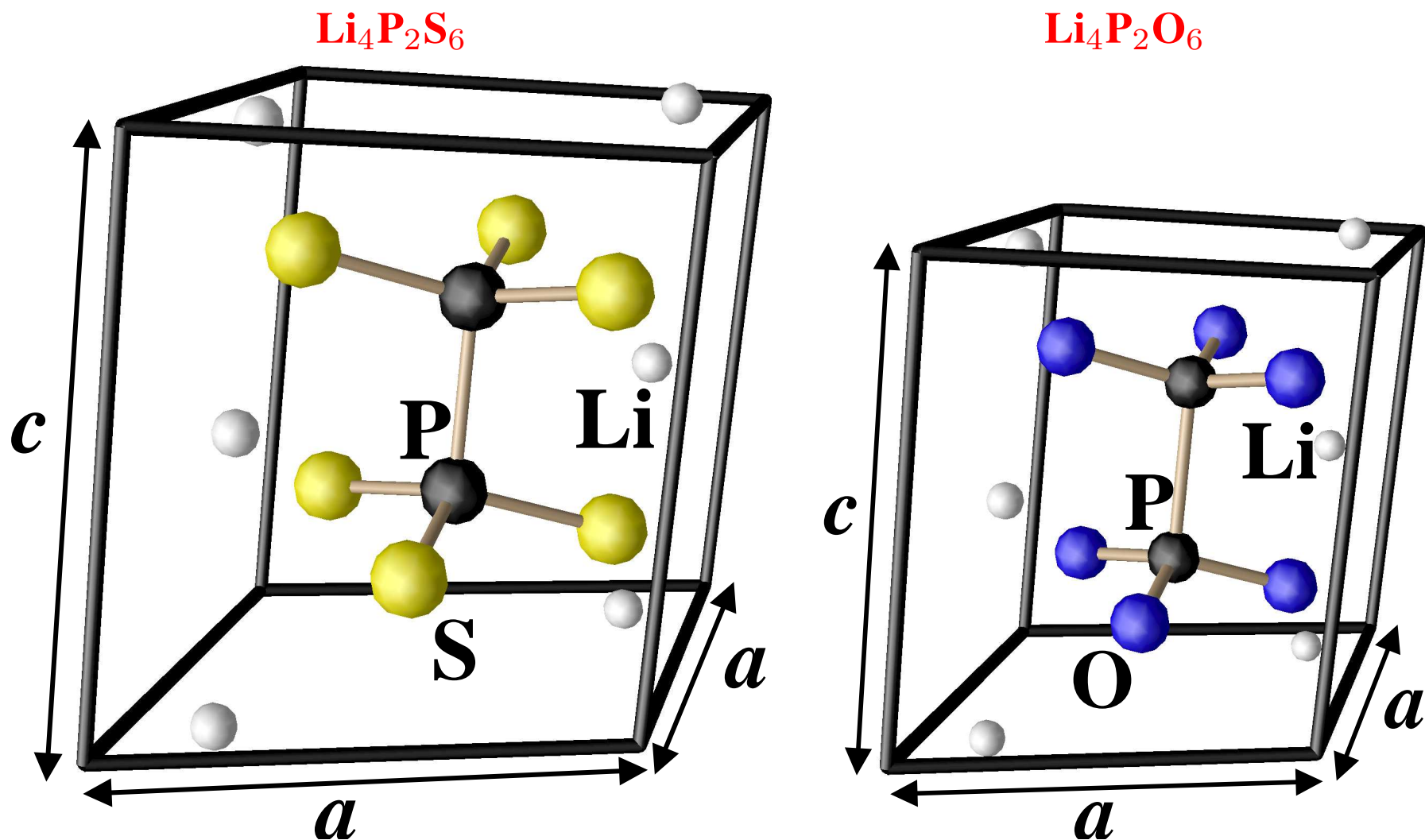


$\beta\text{-Li}_3\text{PO}_4$



Note: $\beta\text{-Li}_3\text{PS}_4$ structure is approximately described as a 125% linear expansion of $\beta\text{-Li}_3\text{PO}_4$. Experiment (Mercier *et al* Acta Cryst. B **38** 1887-1890 (1982)) finds Li_3PS_4 to have Pnma symmetry with fractional occupancy of Li sites. Calculations estimate this structure to be 0.1 eV higher in energy than $\beta\text{-Li}_3\text{PS}_4$.

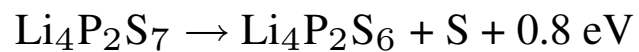
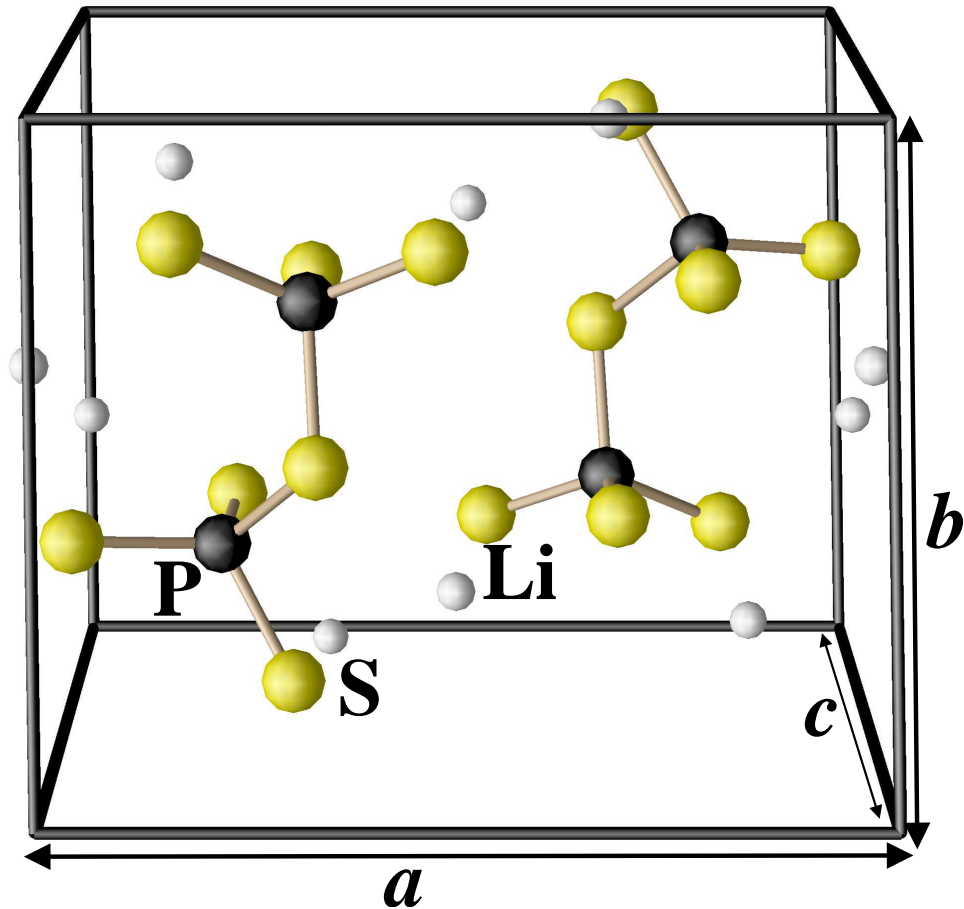
Structural Motifs – $\text{Li}_4\text{P}_2\text{S}_6$ and $\text{Li}_4\text{P}_2\text{O}_6$



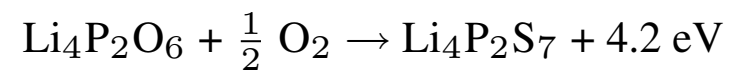
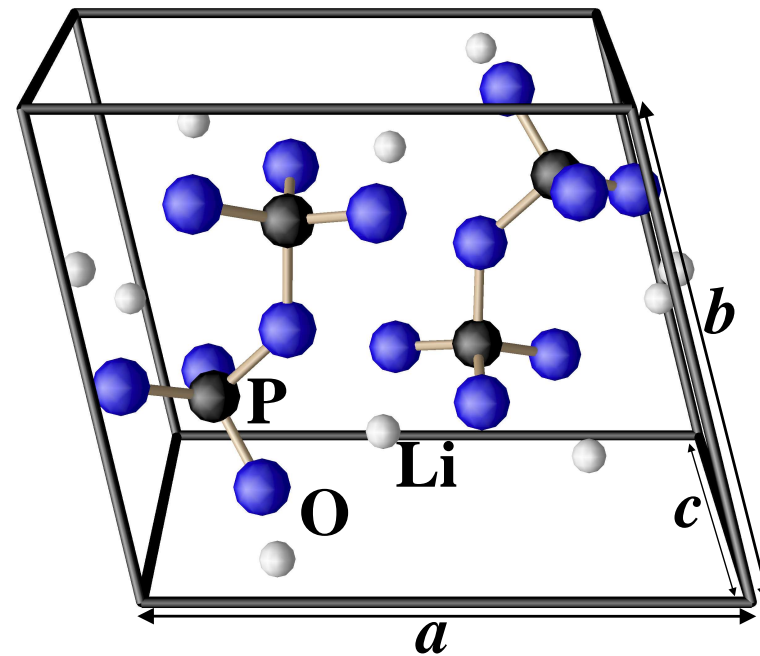
Note: Our optimized structure of $\text{Li}_4\text{P}_2\text{S}_6$ finds the lowest energy to have $\text{P}\bar{3}1\text{m}$ symmetry, a subgroup of the experimental structure (Mercier *et al*, J. Solid State Chem. **43** 151-162 (1982)). The meta-stable $\text{Li}_4\text{P}_2\text{O}_6$ structure can be approximately described as a 80% linear contraction of $\text{Li}_4\text{P}_2\text{S}_6$.

Structural Motifs – $\text{Li}_4\text{P}_2\text{S}_7$ and $\text{Li}_4\text{P}_2\text{O}_7$

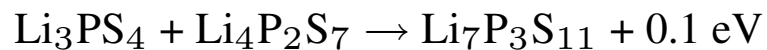
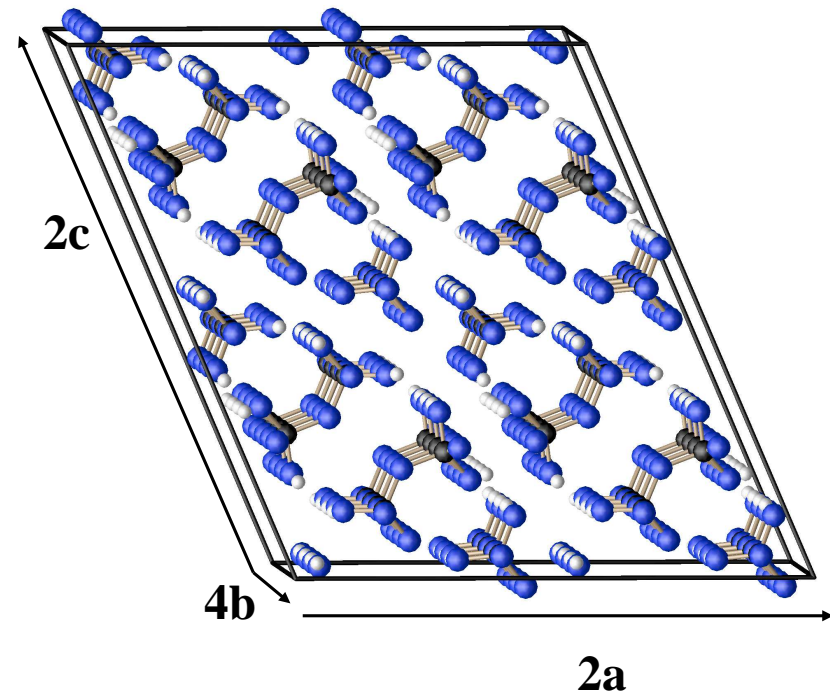
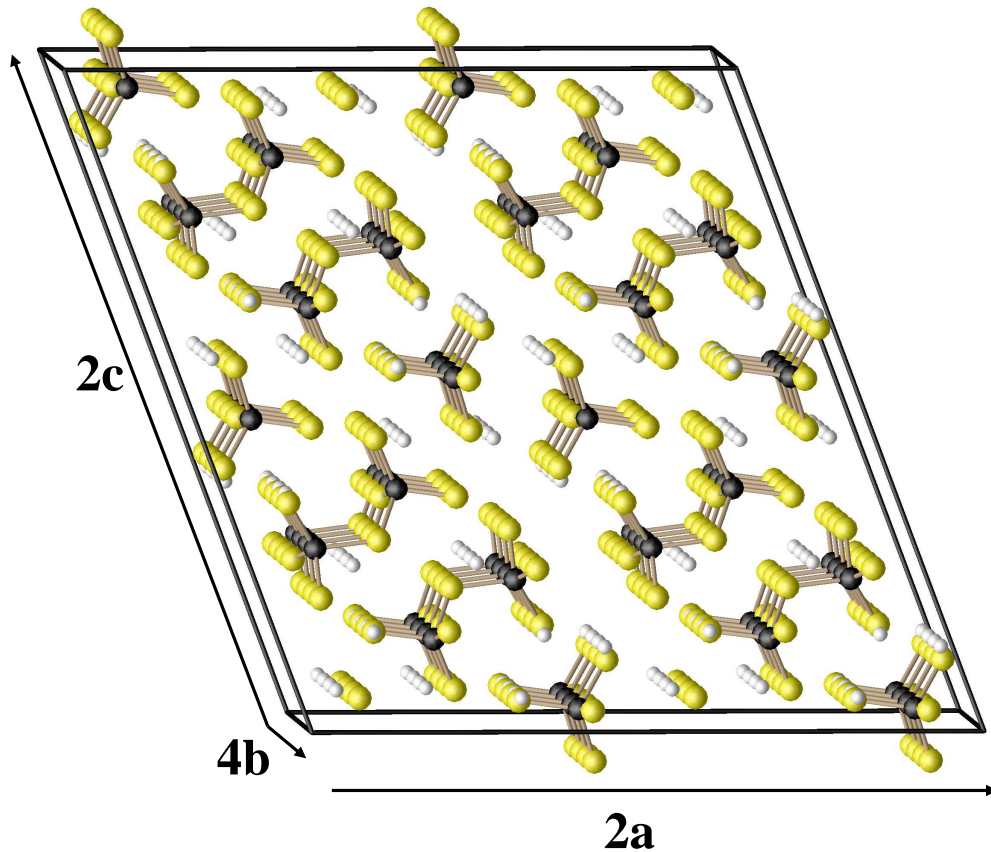
$\text{Li}_4\text{P}_2\text{S}_7$



$\text{Li}_4\text{P}_2\text{O}_7$

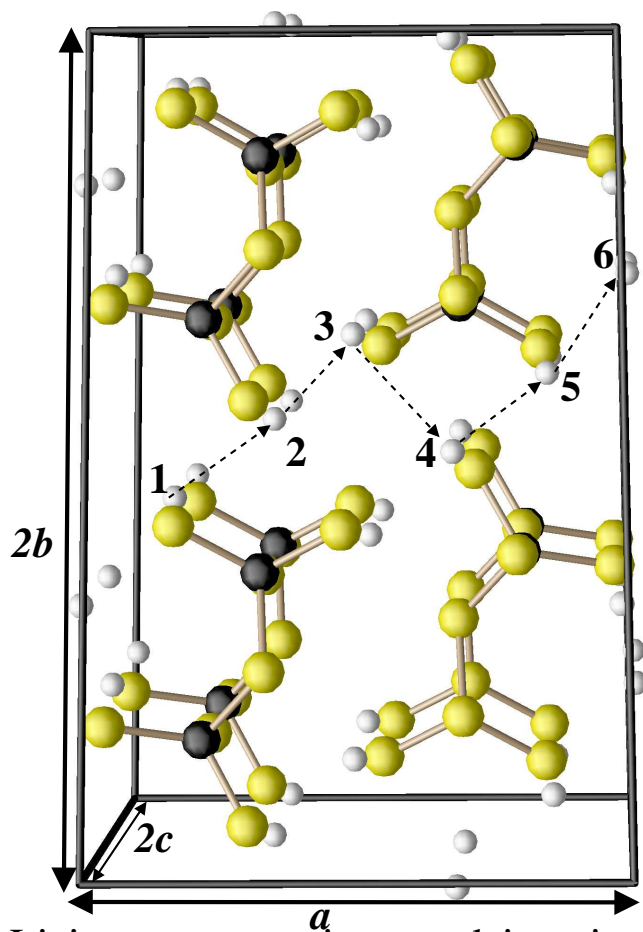


Structural Motifs – $\text{Li}_7\text{P}_3\text{S}_{11}$ and $\text{Li}_7\text{P}_3\text{O}_{11}$

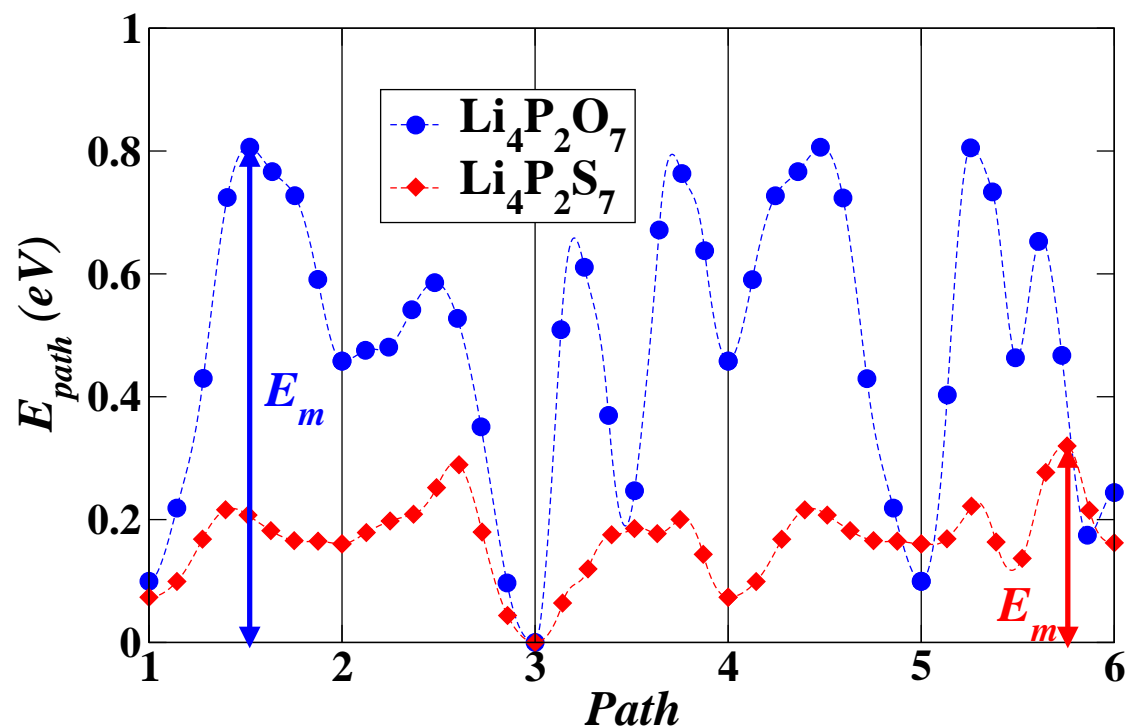


Crystal structure from: Yamane *et al.*, Solid State Ionics **178**, 1163-1167 (2007).

Li⁺ vacancy migration in Li₄P₂S₇ and Li₄P₂O₇

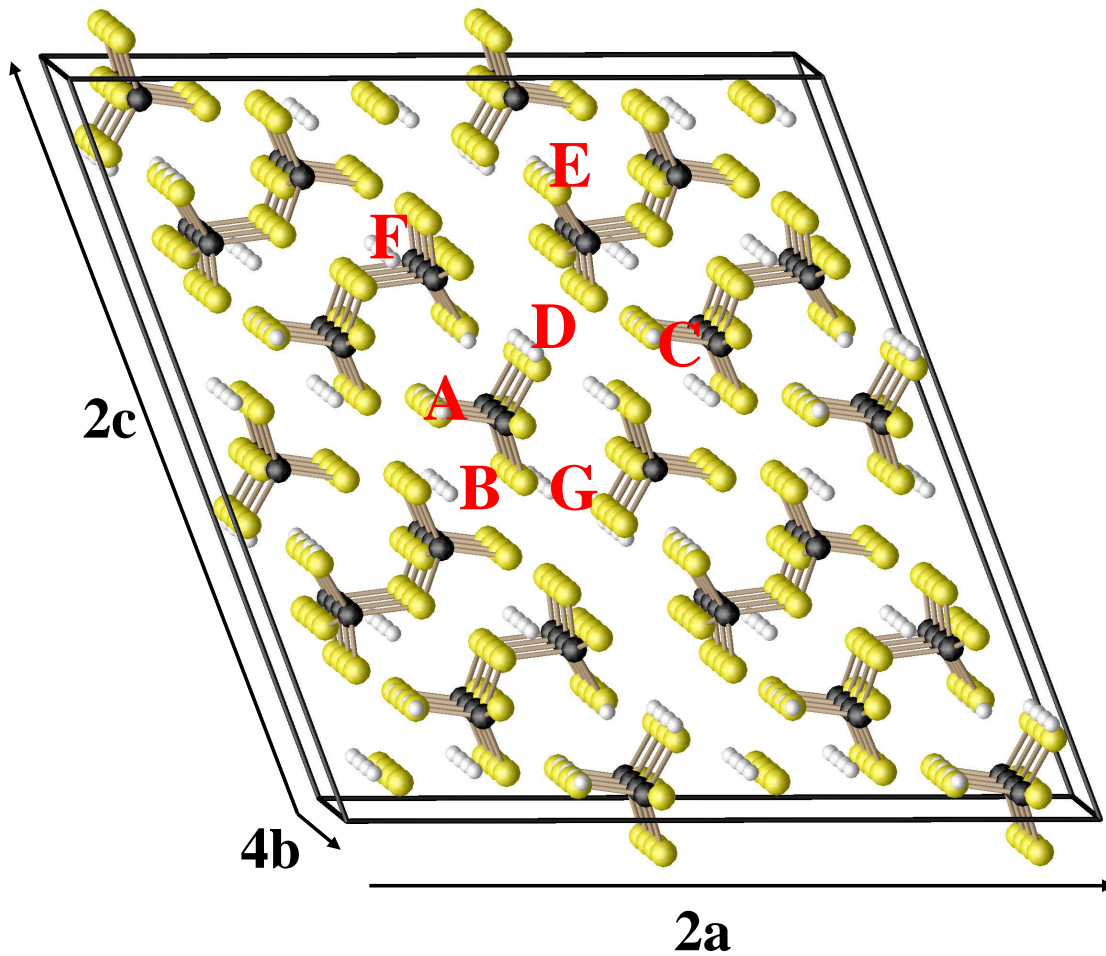


Li ion vacancy sites used in migration energy study for Li₄P₂S₇. Similar sites were used for Li₄P₂O₇.



Energy path diagram for Li ion vacancy migration calculated using the NEB method. For Li₄P₂S₇: $E_m = 0.3$ eV. For Li₄P₂O₇: $E_m = 0.8$ eV

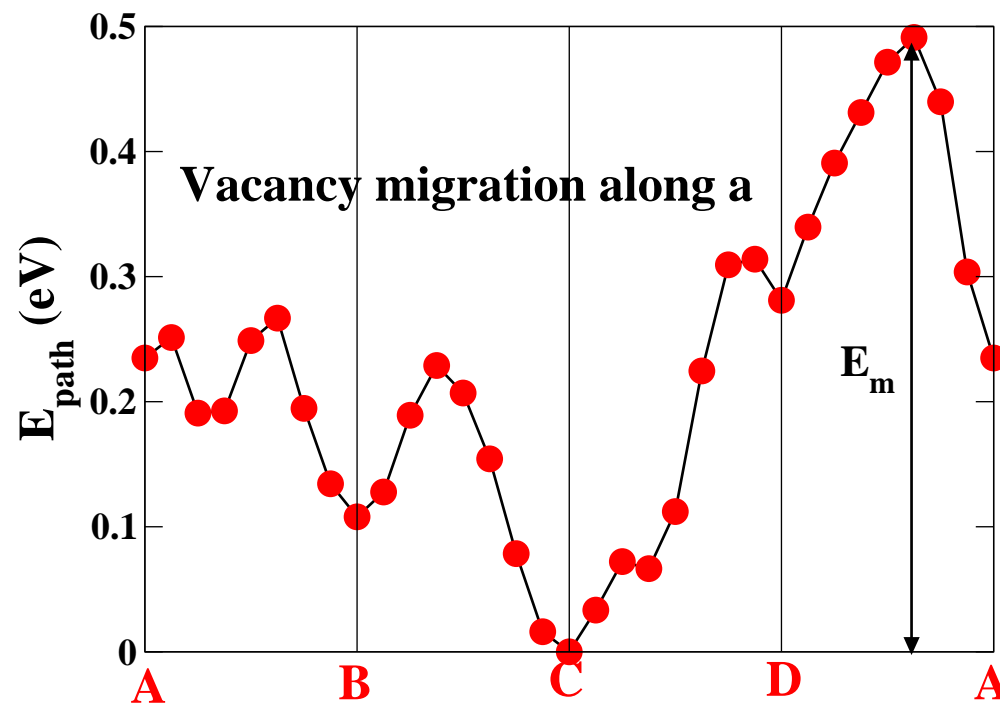
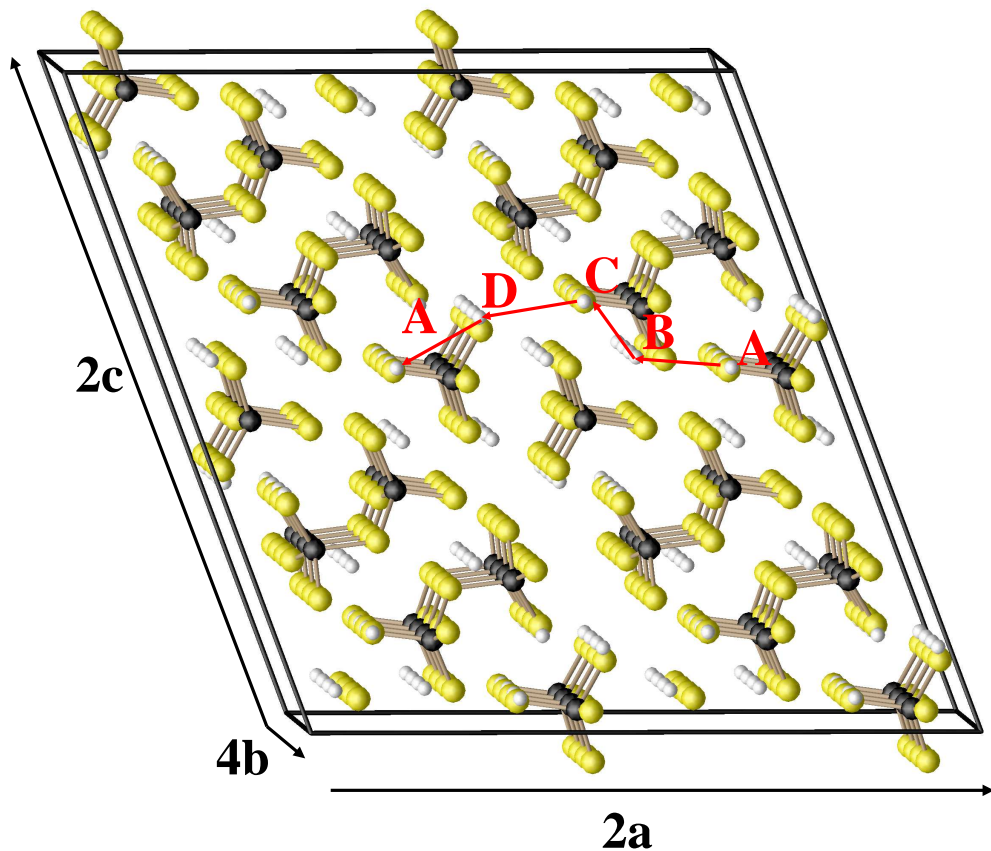
Li ion vacancy sites in $\text{Li}_7\text{P}_3\text{S}_{11}$



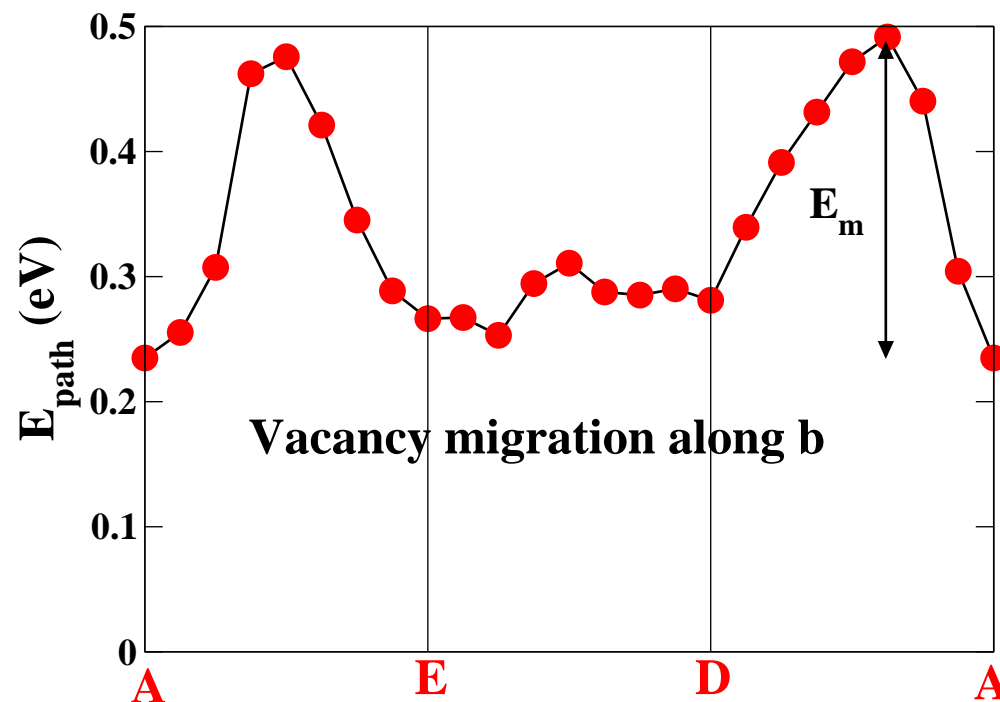
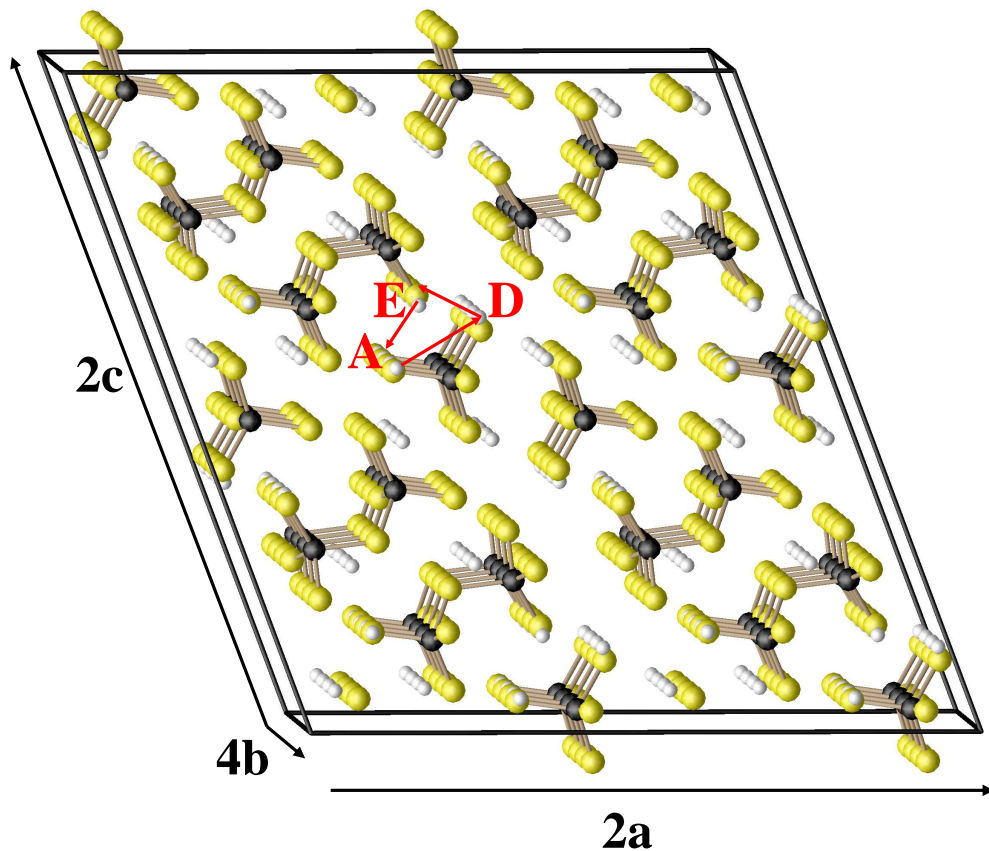
Relative Energies

Label	Energy (eV)
C	0.00
F	0.07
B	0.11
A	0.23
G	0.24
E	0.27
D	0.28

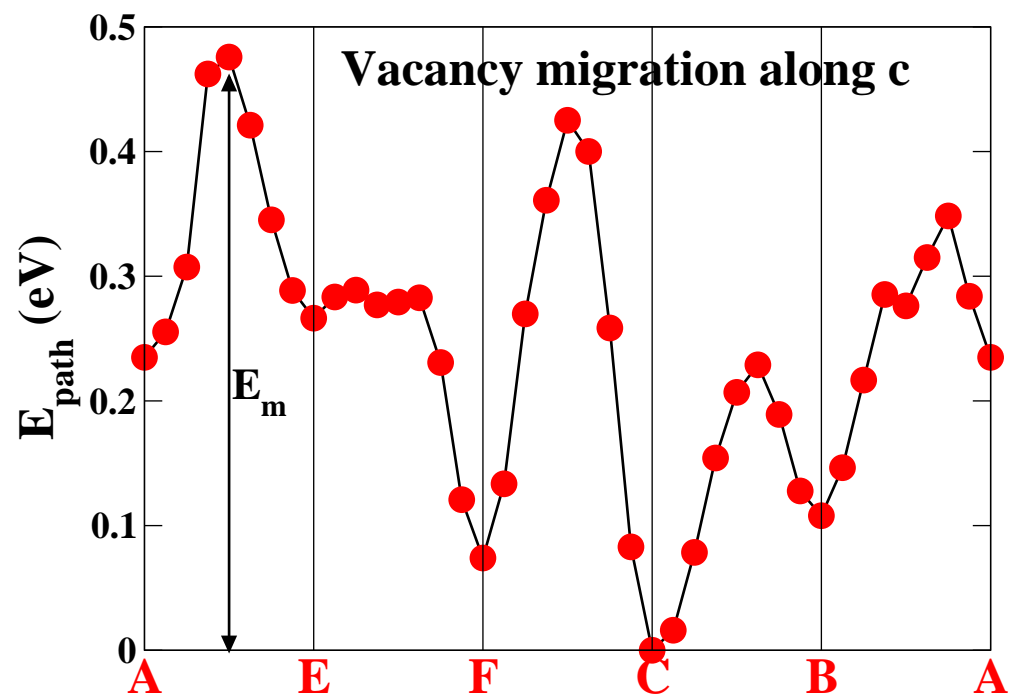
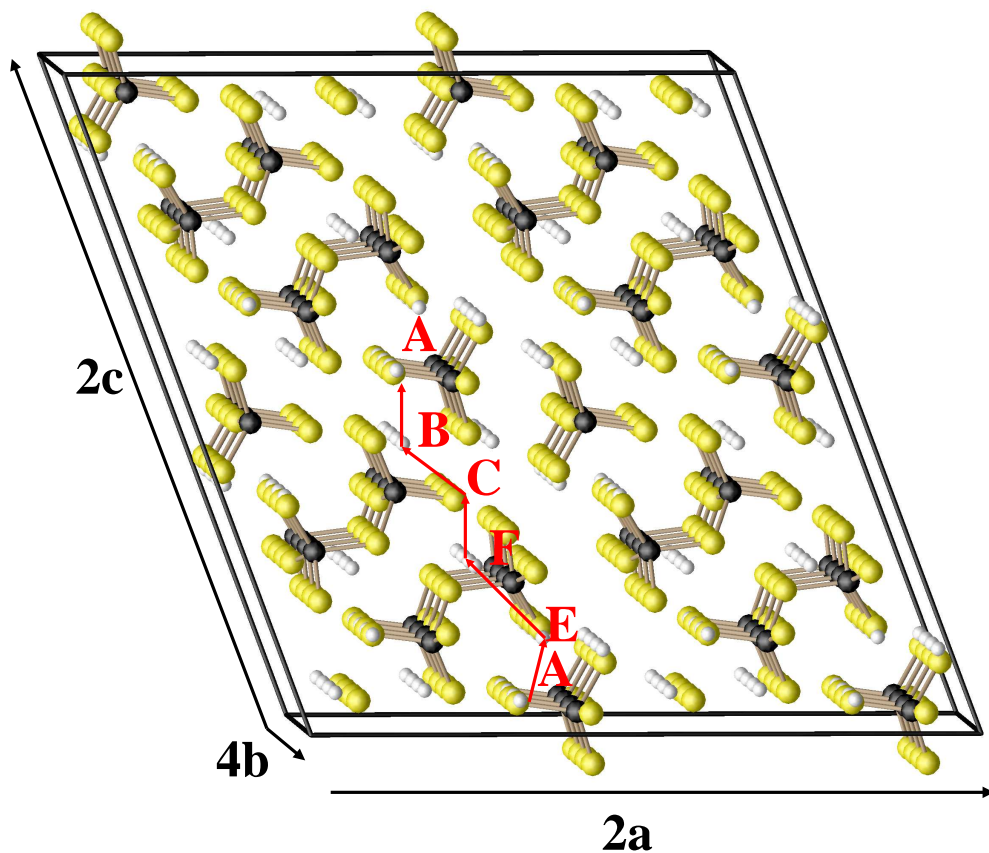
Li ion vacancy diffusion in $\text{Li}_7\text{P}_3\text{S}_{11}$ – a-axis



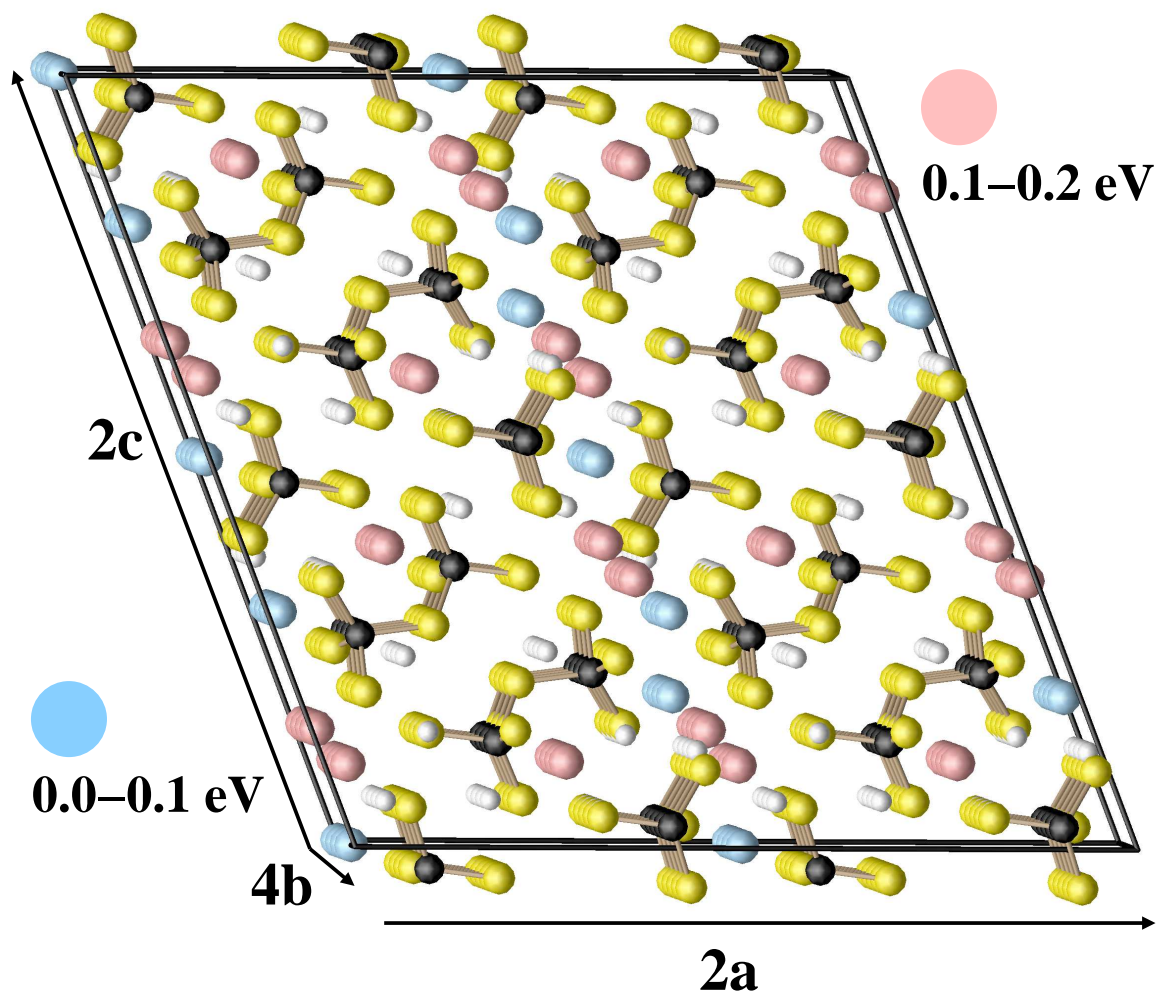
Li ion vacancy diffusion in $\text{Li}_7\text{P}_3\text{S}_{11}$ – b-axis



Li ion vacancy diffusion in $\text{Li}_7\text{P}_3\text{S}_{11}$ – c-axis



Some metastable Li ion interstitial sites in $\text{Li}_7\text{P}_3\text{S}_{11}$



Summary and conclusions

- We have investigated several crystalline Li (thio)phosphates, finding several corresponding stable and meta-stable structures.
- For the example of $\text{Li}_4\text{P}_2\text{S}_7$ and $\text{Li}_4\text{P}_2\text{O}_7$, Li^+ vacancy migration is found to have a smaller migration energy E_m in the thiophosphate (0.3 eV) than in the phosphate (0.8 eV). (Holzwarth, Lepley, and Du, J. Power Sources (2010), doi:10.1016/j.jpowsour.2010.08.042)
- For the "superionic" conductor $\text{Li}_7\text{P}_3\text{S}_{11}$ we have found a Li^+ vacancy migration paths along the **a**, **b**, and **c** directions with migration barriers of 0.5 eV, 0.3 eV, and 0.5 eV respectively. Further work is needed to investigate Li^+ migration via interstitial and/or hybrid mechanisms which is likely to be important in the "super" ionic conduction.
- Work planned for the future includes computational studies of Li phosphate and thiophosphate alloys and continued studies of related solid electrolytes.